行政院國家科學委員會補助專題研究計畫成果報告

※※※※※※※※※※※※※※※※※※※※※※※※※※
※ 黑潮上游海區海洋動力學實驗－子計畫五： ※
※ ※
※ 黑潮上游渦流之形成機制及其對下游之影響－數值模擬研究(II) ※
※※※※※※※※※※※※※※※※※※※※※※※※※※

計畫類別：□個別型計畫　☑整合型計畫

計畫編號：NSC 89－2611－M－002－033－OP2

執行期間：89年8月1日至90年7月31日

計畫主持人：詹森

共同主持人：

本成果報告包括以下應繳交之附件：

□赴國外出差或研習心得報告一份

□赴大陸地區出差或研習心得報告一份

□出席國際學術會議心得報告及發表之論文各一份

□國際合作研究計畫國外研究報告書一份

執行單位：國立台灣大學海洋研究所

中華民國91年1月16日

Seasonal variation of volume transport in the major inflow region of the Taiwan Strait: The Penghu Channel

Sen Jan[1,*], Shenn-Yu Chao[2], and Yu-Huai Wang[3]

[1]National Center for Ocean Research

P. O. Box 23-13, Taipei 10617, Taiwan, R.O.C.

Tel: 886-2-23640917 Fax: 886-2-23644049 email: jansen@odb03.ncor.ntu.edu.tw

[2]Horn Point Laboratory, University of Maryland Center for Environmental Science

P.O. Box 0775, Cambridge, Maryland 21613-0775, U.S.A.

Tel: 410-221-8200 Fax: 410-221-8490 email: chao@hpl.umces.edu

[3]National Center for Ocean Research

P. O. Box 23-13, Taipei 10617, Taiwan, R.O.C.

Tel: 886-2-23640918 Fax: 886-2-23644049 email: yhwang@ccms.ntu.edu.tw

*Corresponding author

Abstract

Eight cruises of current measurements along a zonal transect (~31.84 km) across the major inflow region of the Taiwan Strait, the Penghu Channel, were carried out using the shipboard Acoustic Doppler Current Profiler (ADCP) during 1999~2001. In each cruise, the measurement was repeated twice along the transect with a time lag of 6 hours and 12 minutes, and the repeated data were averaged to eliminate the dominant semidiurnal tidal currents. Velocities after removing semidiurnal tides suggest that there is a strong northward flow centered in the channel, with a speed of about 100 cm/s in the upper 50 m in summer. The northward flow becomes much weaker in winter. The calculated throughflow transports vary seasonally and are correlated with the change of the East Asia monsoon. The estimated transport is around 0 during the peak northeast monsoon in winter, increases from 0.5 to 1 Sv (1 Sv = 10^6 m^3/s) as the northeast monsoon weakens in spring, peaks to 1.5 Sv at the end of southwest monsoon in summer, and decreases rapidly from 1.5 to 0 Sv when the northeast monsoon intensifies in fall. The error induced by unfiltered diurnal tidal currents is estimated to be about $\pm$ 0.20 Sv in the transport calculation.

(Keywords: Penghu Channel, throughflow transport, shipboard ADCP)

1. Introduction

The Penghu Channel (PHC), bounded by the Penghu Islands and Taiwan Banks to the west and the southwest coast of Taiwan to the east, is a funnel-shaped deep channel. Located off southwest Taiwan, it is about 40 km wide and 100 m deep to the north, and 80 km wide and 200 m deep to the south (Fig. 1). It is well known that there is a persistent northward flow in the PHC throughout a year (Chuang, 1985; 1986). Analyses based on hydrographic data (Wang and Chern, 1988 and 1992; Xiao and Cai, 1988) suggest that the northward flow is the major inflow entering the Taiwan Strait. The inflow is often speculated to be the origin of the so-called "Taiwan Current" (Guan, 1986). Recent current measurements using the shipboard Acoustic Doppler Current Profiler (ADCP) over zonal transects east and west of the Penghu Islands further suggest that transport through the PHC amounts to about 60% of the total volumetric influx entering the Taiwan Strait in summer (Wang, 1999). Using a numerical model driven by throughflow transports estimated by Wyrtki (1961), Jan et al. (2000) indicated that the transport through the PHC controls the seasonal variation of the circulation in the Taiwan Strait. Farther to the north, the Taiwan Strait outflow has been inferred to be an important source to the nutrient balance over the East China Sea (Liu, 2000). In addition, Katoh et al. (2000) emphasized the importance to monitor the fluctuations of the Taiwan Current and the Kuroshio Branch Current in order to

determine the variability of the Tsushima Current.

It is clear that the throughflow transport in the PHC is important not only to the circulation patterns in the Taiwan Strait, but also to the balance of biogeochemical budget in the East China Sea. Unfortunately, estimates of the transport are scanty in the open literature. Wyrtki (1961) might have provided the earliest estimate of transports through the Taiwan Strait. His strait-wide transport estimate is not the same as the transport through the PHC, but the two share a significant common component. His rough estimates of 0.5-1 Sv (1 Sv = 10^6 m^3/s) northward in summer and 0.5 Sv southward in winter captured the seasonal trend of the PHC transport to lowest order. Chuang (1986) measured the current in the PHC using a current meter moored about 20 m above the bottom, and found a northward mean flow of 32 cm/s in spring. Using this result (Chuang, 1986), Fang et al. (1991) speculated that the transport from the Penghu Islands to Taiwan is 0.4 Sv northward in winter (December-May). Using the same result (Chuang, 1986), Jan et al. (2000) estimated that the transport through the PHC is at least 1 Sv in summer. The inconsistency is evident and points out the need for better estimates.

Because of the lack of direct current measurements, the aforementioned estimates are too coarse in space and time to determine the transport through the PHC and its seasonality. In light of these uncertainties, the objective of this study simply aims to

measure the currents and calculate the throughflow transport in the PHC directly. The shipboard ADCP was used for the measurement. The cruise track was designed for the purpose of eliminating the dominant semidiurnal tidal currents, and the phase average was used for data processing. Eight cruises of measurement were performed during 1999-2001. Results obtained from the measurements are expected of useful for improving the numerical model results for the Taiwan Strait, and relevant calculation of biogeochemical fluxes from the Taiwan Strait to the East China Sea. The observational results are presented and discussed below.

2. Observations

Eight cruises of measurements were conducted on board Ocean Research I and III (OR-1 and OR-3) along a zonal transect across the width of northern PHC [line A-B in Fig. 1(b)] during 1999~2001. The transect is about 31.84 km long. Table 1 lists the period of each measurement. The velocities were measured using the shipboard ADCP manufactured by RD Instruments with 150 kHz and 75 kHz for OR-1 and OR-3, respectively. The velocity of each cast is averaged every 8 m in the vertical, and the blanking depth is 12 m below the sea surface. The bottom-tracking mode of the ADCP was used during the measurement.

According to the velocities measured at a station 50 km north of the transect

[station P in Fig. 1(b)], tidal currents are predominantly semidiurnal in the PHC. Fig. 2 shows an energy spectrum of the depth-averaged velocities measured at station P from October 25 1999 to March 24 2000. The main peak of the spectral density for the north-south (v) component occurs at the semidiurnal and diurnal tidal frequencies. The formal is greater than the latter by two orders of magnitude. The tidal current energy of zonal (u) component is relatively small compared to that of the v-component. Harmonic analysis suggests that tidal current amplitudes of O_1, K_1, N_2, M_2 and S_2 for the dominant v-component are 4, 7, 13, 67 and 20 cm/s, respectively. The corresponding phases are 342°, 12°, 321°, 345° and 22°. These indicate that the amplitude of diurnal tidal current is only about one tenth of that of the semidiurnal tidal current. Tidal current ellipses (not shown) suggest that the major axis is aligned along the major axis of PHC.

Because of the limited availability of ship time, the ship track was designed so as to eliminate only the dominant semidiurnal tidal currents. We made the current measurements along the same transect twice, i.e., the first and third tracks as illustrated in Fig. 3. The two repeats are separated by 6 hours and 12 minutes so that they are out of phase by half a cycle of the semidiurnal tides. Ship speed was controlled at speed of 5-6 knots (1 knot = 0.514 m/s) so as to maintain the data quality of the measurement (Tang and Ma, 1995). It took 3 hours and 6 minutes to complete measurements from one end of the transect to the other. In case of limited ship availability, this observation method

is often used for the mean flow measurement and transport estimation (e.g., Katoh et al., 1996 and 2000; Liu et al., 2000).

As for data processing, the velocity data along the transect are separated to eight segments and averaged over each segment (Fig. 3). This may reduce instrument errors but also decrease the horizontal resolution of data. The segment-averaged velocity is assigned at the midpoint of each segment. The segment-averaged data are further gridded every 4 m in the vertical from the surface down to near bottom by solving

$$(1-\alpha)\cdot\ \nabla(\nabla\phi) + \alpha\cdot\ \nabla\phi = 0 \qquad (1)$$

where ϕ represents velocity components u or v, ∇ represents the Laplacian operator defined as $i(\partial/\partial x) + k(\partial/\partial z)$, and α is a tension factor; $\alpha = 0.6$ provides the best fit of original data. The resulting velocity is assigned to the center of each layer. The bottom depths for gridding are cut at 68, 60, 76, 108, 108, 120, 92 and 52 m for the eight segments from west to east. The horizontal velocity is assumed to be zero at the bottom. The gridded data of the first and third tracks were averaged to eliminate the semidiurnal tidal currents. This procedure is so-called "phase averaging". The phase-averaged current is referred to as the "semidiurnally averaged current" hereafter. The volume transport through the transect (Q_{PHC}) is calculated using the semidiurnally averaged velocity perpendicular to the transect as

$$Q_{PHC} = \sum_{i=1}^{8}\sum_{k=1}^{K_i} v_{i,k}\cdot(\delta z\cdot d) \qquad (2)$$

where $d = 3.98$ km is the width of each segment, i is the segment number, k is the layer index, K_i is bottom layer index of the ith segment, and $\delta z = 4$ m is the layer thickness.

For further data analysis, we also obtained the wind data of an island weather station [DG in Fig. 1(b)] from the Central Weather Bureau of Taiwan.

3. Results

To facilitate discussions below, it is more practical to follow changes of monsoon winds to define winter, spring, summer and fall as periods from November to February, March to May, June to August and September to October, respectively (Jan et al., 2000). Fig. 4 shows the semidiurnally averaged velocity contours of the u- and v-components in the transect from the eight measurements. The flow velocities are essentially northward in the transect and vary seasonally. By comparison, zonal currents (u-component) are much weaker. The northward currents are weak (<10 cm/s) in winter [Fig. 4(c) and (g)]. During the winter-spring transition period [Fig. 4(d)], the flow field develops a core structure centered in the middle of the transect; the northward velocity in the upper 50 m layer increases (>20 cm/s) thereafter. In late summer [Fig. 4(a) and (f)], the northward flow core is fully developed and its speed can be as high as 100 cm/s. After summer, the northward flow strength decreases rapidly, and the core speed is reduced to about 50 cm/s [Fig. 4(b)]. The near bottom velocities presented in Fig. 4(d)

and (h) are close to that (32 cm/s) observed by Chuang (1986) in March-April of 1985.

The depth-averaged distributions of the semidiurnally averaged currents along the transect are shown in Fig. 5. The strength of velocity vectors clearly peaks over the deepest region of the transect in summer [Fig. 5(a), (e) and (f)], and decreases in spring and fall to about half of the summer peak [Fig. 5(b), (d) and (h)]. In contrast, the winter flow is much weaker and less coherent [Fig. 5(c) and (g)]. Both Figs. 4 and 5 reveal that there is a strong northward flow (~100 cm/s) through the PHC during summer, whereas the semidiurnally averaged flow is nearly stagnant during winter.

The volume transports calculated from the velocities acquired in the eight measurements listed in Table 1 are 1.58, 0.76, -0.11, 0.56, 1.26, 1.72, 0.02, and 1.10 Sv, respectively. Expected errors in the transport calculation are mostly induced by the diurnal tidal currents that cannot be fully eliminated through the semidiurnal averaging of the measured velocities. The velocity of the diurnal currents may be comparable to that of the subtidal currents when the flow is weak, though the diurnal currents are quite small compared to the semidiurnal currents. The instrument error, the mathematical methods using in data interpolation and discrete area integration for velocity, etc., might introduce errors in the transport calculation but are expected to be minor in comparison with that from the unfiltered diurnal tidal currents. We estimate the major error induced by the diurnal currents as follows. The harmonic constants of tidal

currents in the PHC indicate that the amplitude of depth-averaged composite diurnal current (O_1+K_1) is about 11 cm/s with the major axis aligned along the longitudinal axis of PHC. Assume that the velocity of depth-averaged diurnal current can be written as $a^*cos(\omega t)$, where t is time, a = 11 cm/s is the amplitude and ω is the frequency of the diurnal current. Applying the semidiurnal averaging to the diurnal currents, the resulting mathematical expression, $0.5^*a^*\{cos(\omega t) + cos[\omega(t + 6.2\ \text{hrs})]\}$, yields the maximum velocity of residual diurnal currents of about 7 cm/s. The consequent error for the calculated volume transport ranges up to about ± 0.20 Sv.

Fig. 6 shows the calculated transports as a function of time, and the daily mean wind speed sticks at an island weather station near the west end of the transect (DG in Fig. 1) from January 1999 to June 2001. The calculated transports vary seasonally and seem to be correlated with the changing winds. The wind sticks as shown in Fig. 6 indicate that winds over this area are dominated by the northeast monsoon. It is likely that the northward transport is mostly offset by the northeast monsoon in winter. The northward transport clearly decreases as the northeast monsoon intensifies. The northward transport may reach its maximum near the end of the southwest summer monsoon.

4. Discussion and concluding remarks

Fig. 6 suggests that the calculated volume transport through the PHC is highly correlated with the variation of local winds. However, the temporal resolution of the calculated transports is still too poor to determine the coherence and phase lag between local winds and transports. In spite of this deficiency, seasonality can still be inferred. Fig. 7 shows the calculated transports as a function of the month regardless the year of measurement, along with the monthly mean wind speed vectors at DG averaged from 1986 to 1997. The local winds are essentially dominated by the East Asia monsoon, from northeast in winter and from southwest in summer. The northeast monsoon begins in mid September, reaches its maximum from October to January, and weakens continuously thereafter. By contrast, the southwest monsoon in June and July is much weaker. The magnitude of northward transport displayed in Fig. 7 is inversely proportional to the strength of the northeasterly wind. In winter, the northeast monsoon severely blocks the northward flow in the PHC, resulting in a nearly zero transport from November to February. In spring, relaxation of northeast monsoon unleashes the northward intrusion of waters from the southeastern Taiwan Strait, and the northward transport mildly increases with time from March to July. With the aid of summer southwest monsoon, the northward transport peaks in August. Since the southwest monsoon is quite weak in summer, a good portion of the throughflow must be forced by remote forcing of large-scale origin rather than by local winds. As the northeast

monsoon starts in fall, the northward flow decreases again and the transport drops rapidly. About two months after the onset of the northeast monsoon, the northward transport reaches its minimum. We estimated that the transport is around 0 in winter, from 0.5 to 1 Sv in spring, 1.5 Sv in summer, and decreasing from 1.5 to nearly 0 Sv from fall to early winter. The seasonal variation of volume transports through the PHC can also be inferred from three-dimensional circulation models by minimizing discrepancies between model outputs and hydrographic data. An attempt along this line had been made by Jan et al. (2000) and the inferred transports are similar to estimates established herein.

According to Wang (1999), the volume transport through PHC amounts to at least three fifths of the summer northward inflow entering the Taiwan Strait. This is quite substantial considering the fact that the width of PHC is only one fifth of that across the southern Taiwan Strait. The semidiurnally averaged currents extracted from the eight measurements suggest that, over the deepest portion of the PHC, there is a quite strong northward velocity core with a speed of ~100 cm/s in the upper 50 m layer in summer. The northward flow becomes much weaker and the high-speed core nearly disappears in winter. The calculated volume transports through the PHC are –0.11~0.02 Sv, 0.56~1.10 Sv, 1.26~1.72 Sv and 0.76 Sv in winter, spring, summer and fall, respectively, suggesting the throughflow in the PHC is generally northward but with strong seasonal

variations. The diurnal tidal currents, which cannot be fully eliminated by the semidiurnal averaging, may cause deviations of ± 0.20 Sv in the transport calculation. These lead to estimates of seasonal mean transport of about 0 in winter, 0.5~1 Sv in spring, 1.5 Sv in summer, and 1.5~0 Sv in fall. The inferred seasonal variation of the transport appears to be highly correlated with changes of the East Asia monsoon. The transport is quite small during the strongest northeast monsoon period in winter from November to February, increases as the northeast monsoon weakens in spring, peaks after the southwest monsoon in summer, and decreases rapidly when the northeast monsoon starts in fall.

Developments of a high-resolution nowcast model for the Taiwan Strait, an East China Sea hydrodynamic model and associated biogeochemical investigations have been underway. Results documented herein provide the crucial input to the aforementioned modeling efforts. At the present time, our transport estimates in the PHC are limited to the seasonal time scale. Current variations below and beyond the seasonal time scales remain to be elucidated. Below the seasonal time scale, the effect of typhoons on the transport warrants further investigations. Beyond the seasonal time scale, inter-annual modulations induced by El Niño needs to be examined. Volume transport across the transect between the mainland China and the Penghu Islands also warrants further measurements. Therefore, the present study serves only as a modest

start toward a long line of future investigations.

Acknowledgements

The National Science Council of the Republic of China supported this work under the project "TSNOW". Professors C.-S. Chern, J. Wang and T.-Y. Tang of Institute of Oceanography, National Taiwan University provided valuable suggestions for this study. Technicians W.-H. Ho, C.-C. Chiou, J.-K. Hu and the crew of Ocean Research I and III assisted the measurement. The Central Weather Bureau kindly provided the wind data. This is the National Center for Ocean Research contribution number #.

References

Chuang, W.-S., 1985. Dynamics of subtidal flow in the Taiwan Strait. Journal of the Oceanographic Society Japan, 41, 65-72.

Chuang, W.-S., 1986. A Note on the Driving Mechanisms of Current in the Taiwan Strait. Journal of the Oceanographic Society Japan, 42, 355-361.

Fang, G., B. Zhao and Y. Zhu, 1991. Water volume transport through the Taiwan Strait and the continental shelf of the East China Sea measured with current meters. In Oceanography of Asian Marginal Seas, edited by K. Takano, pp. 345-358, Elsevier, New York

Guan, B., 1986, A sketch of the current structures and eddy characteristics in the East China Sea. Studia Marina Sinica, 27, 1-20 (in Chinese with English abstract)

Jan, S., J. Wang, C.-S. Chern and S.-Y. Chao, 2000. Seasonal variation of the circulation in the Taiwan Strait. Journal of Marine Systems. (in review)

Katoh, O., K. Teshima, O. Abe, H. Fujita, K. Miyaji, K. Morinaga, and N. Nakagawa, 1996. Process of the Tsushima Current formation revealed by ADCP measurements in summer. Journal of Oceanography, 52, 491-507.

Katoh, O., K. Morinaga and N. Nakagawa, 2000. Current distributions in the southern East China Sea in summer. Journal of Geophysical Research, 105, C4, 8565-8573

Liu, K.-K., T.-Y. Tang, G.-C. Gong, L.-Y. Chen and F.-K. Shiah, 2000. Cross-shelf and along-shelf nutrient fluxes derived from flow fields and chemical hydrography observed in the southern East China Sea off northern Taiwan. Continental Shelf Research, 20, 493-523

Tang, T.-Y. and J.-C. Ma, 1995. A note on the accuracy of shipboard ADCP on Ocean Research I. Acta Oceanographica Taiwanica, 34, 71-81

Wang, J. and C.-S. Chern, 1988. On the Kuroshio branch in the Taiwan Strait during wintertime. Progressive Oceanography, 21, 469-491.

Wang, J. and C.-S. Chern, 1992. On the distribution of bottom cold waters in Taiwan Strait during summertime. La mer 30, 213-221

Wang, Y.-H, 1999. Volume transport observations in the Taiwan Strait. Abstracts of 1999 Ocean Science Meeting , Taiwan. 203-204

Wyrtki, K., 1961. Physical oceanography of the southeast Asia waters. Scientific results of marine investigations of the South China Sea and Gulf of Thailand. 1959-1961, Naga Report, 195pp.

Xiao, H. and S. Cai, 1988. Distribution characters of sea temperature and salinity in western Taiwan Strait. Journal of Oceanography in Taiwan Strait, 7, 3, 227-234 (in Chinese with English abstract)

Figure captions:

Fig. 1 Maps showing (a) topography in the Taiwan Strait, and (b) the ship track of velocity measurements across the Penghu Channel.

Fig. 2 Power spectrum of the depth-averaged velocities measured at a mooring station P about 50 km north of the transect (see Fig. 1) from October 25 1999 to March 24 2000. The dashed and solid lines are the spectral density of the zonal (u-) and meridional (v-) velocity components, respectively.

Fig. 3 Schematic showing the track of shipboard ADCP measurement as a function of time. The velocities acquired on each track were equally divided to eight segments and were averaged over each segment.

Fig. 4 Semidiurnal-averaged velocity contours (u and v components) in the transect for the eight measurements. Contour interval is 10 cm/s.

Fig. 5 Horizontal distribution of the depth-averaged velocities calculated from the semidiurnal-averaged currents along the track for the eight measurements.

Fig. 6 (a) daily mean wind speed sticks at an island weather station DG (see Fig. 1) from January 1999 to June 2001, and (b) calculated volume transports as a function of time.

Fig. 7 (a) monthly mean wind speed vectors at DG averaged from 1986 to 1997, and (b) calculated transports over a one-year time scale regardless the year of measurement.

Table 1 Shipboard ADCP measurement periods and the calculated throughflow transport for the eight cruises. The transport is in Sv (10^6 m^3/s) with positive transports toward the north.

R/V	Cruise no.	Measurement period	Q_{PHC} (Sv)
OR-1	558	1999/08/15/14:00-22:42	1.58
OR-3	569	1999/10/15/19:00-16/04:23	0.76
OR-1	569	1999/11/19/04:00-13:30	-0.11
OR-1	578	2000/03/24/21:00-25/07:46	0.56
OR-1	585	2000/06/18/01:50-11:10	1.26
OR-3	646	2000/08/18/13:15-22:40	1.72
OR-1	602	2001/02/12/09:22-19:00	0.02
OR-3	702	2001/05/24/09:38-18:56	1.10

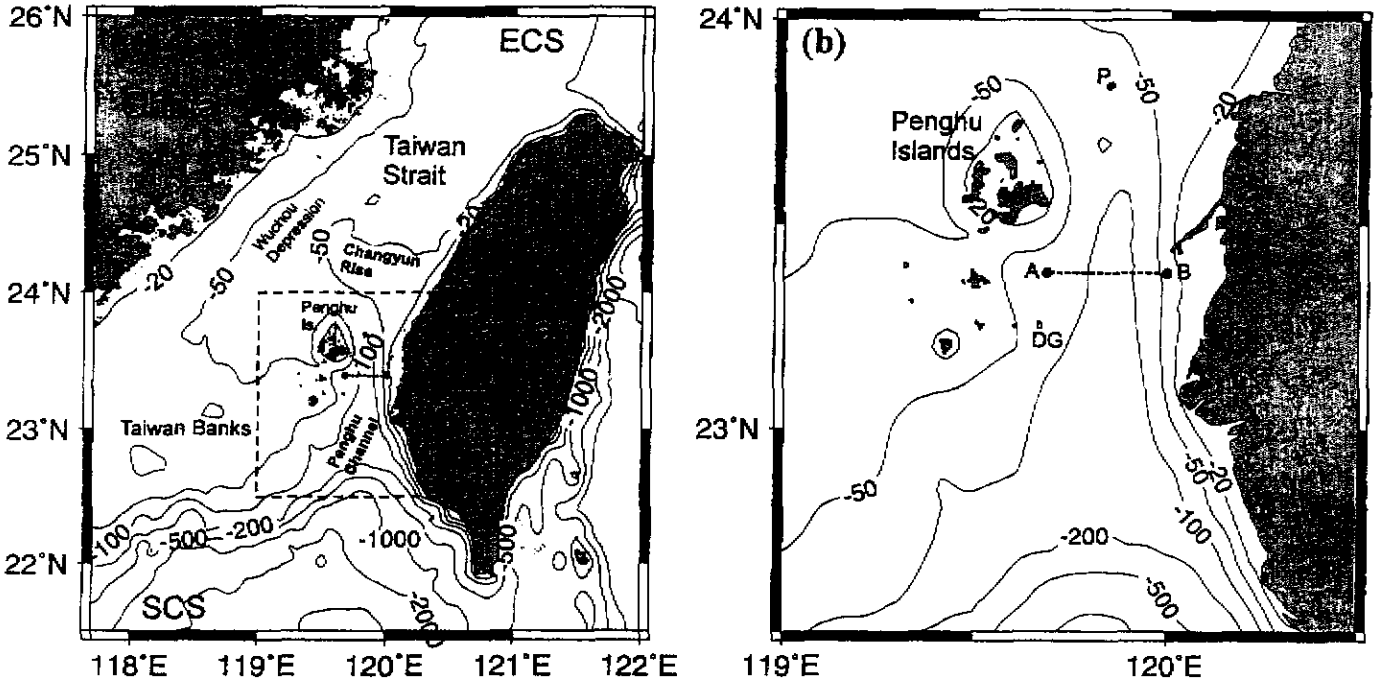

Jan, Chao and Wang Fig. 1

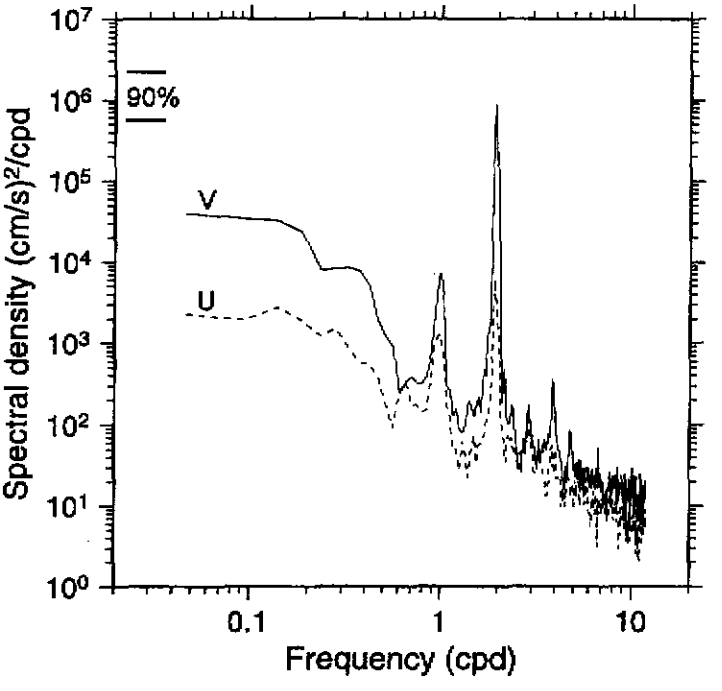

Jan, Chao and Wang Fig. 2

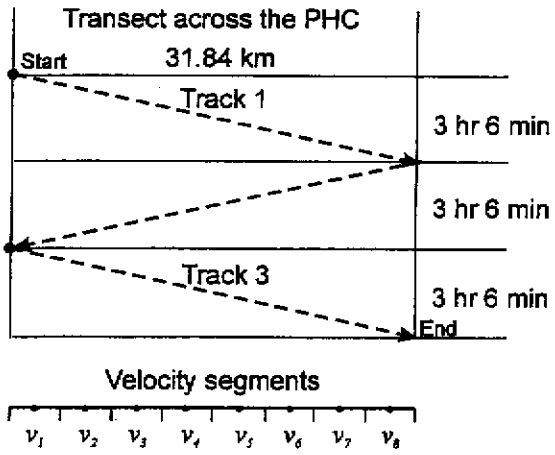

Jan, Chao and Wang Fig. 3

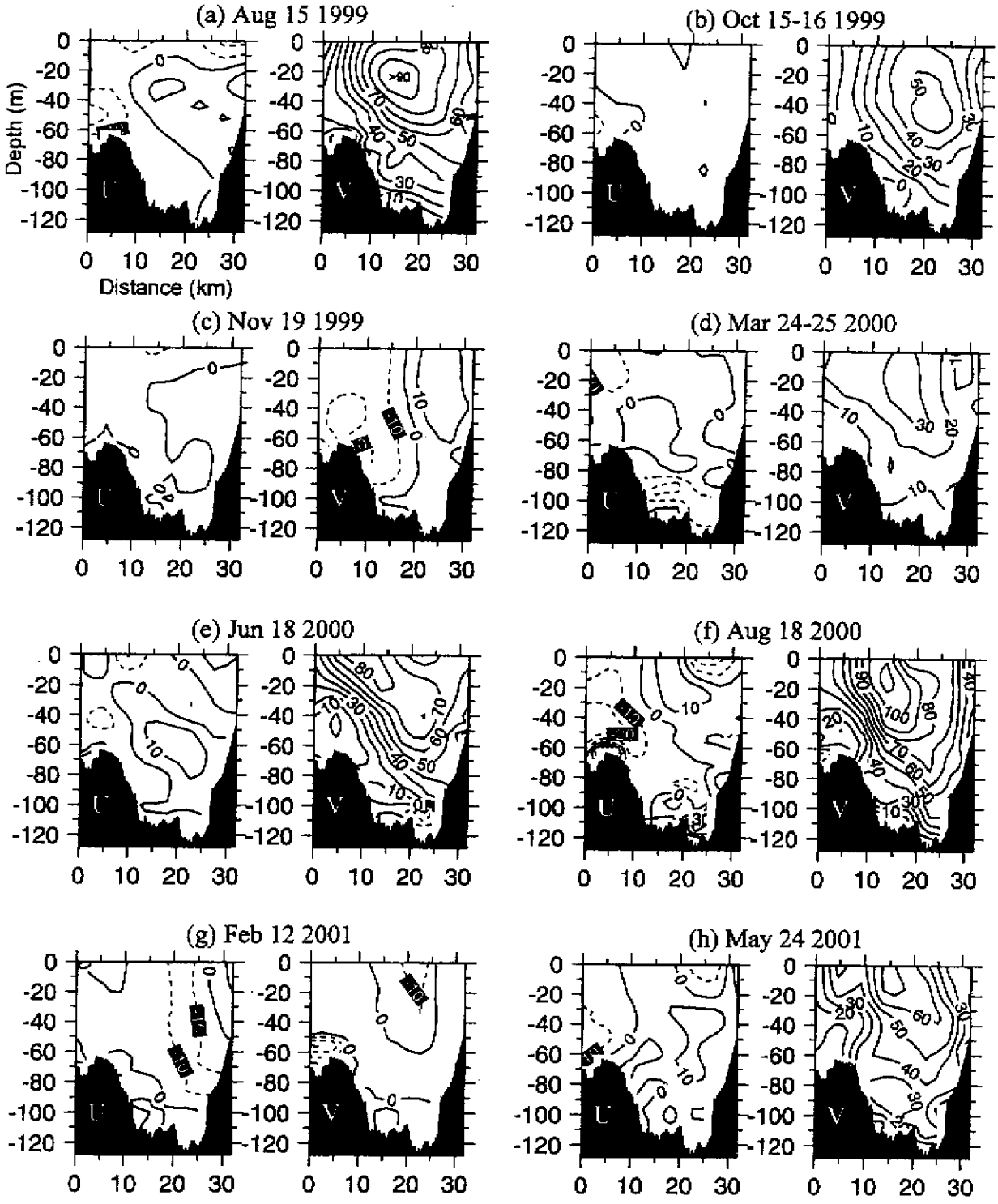

Jan, Chao and Wang Fig. 4

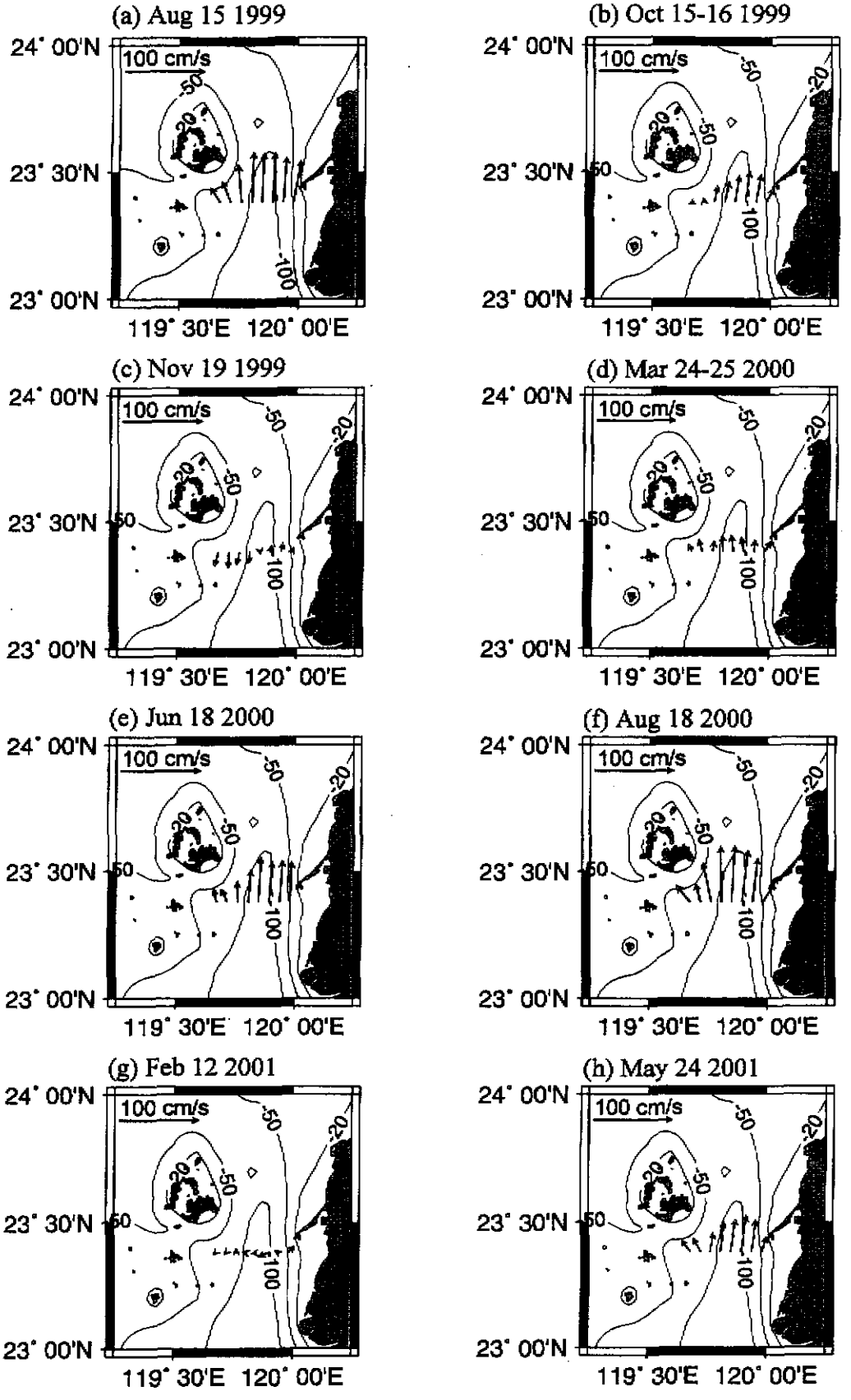

Jan, Chao and Wang Fig. 5

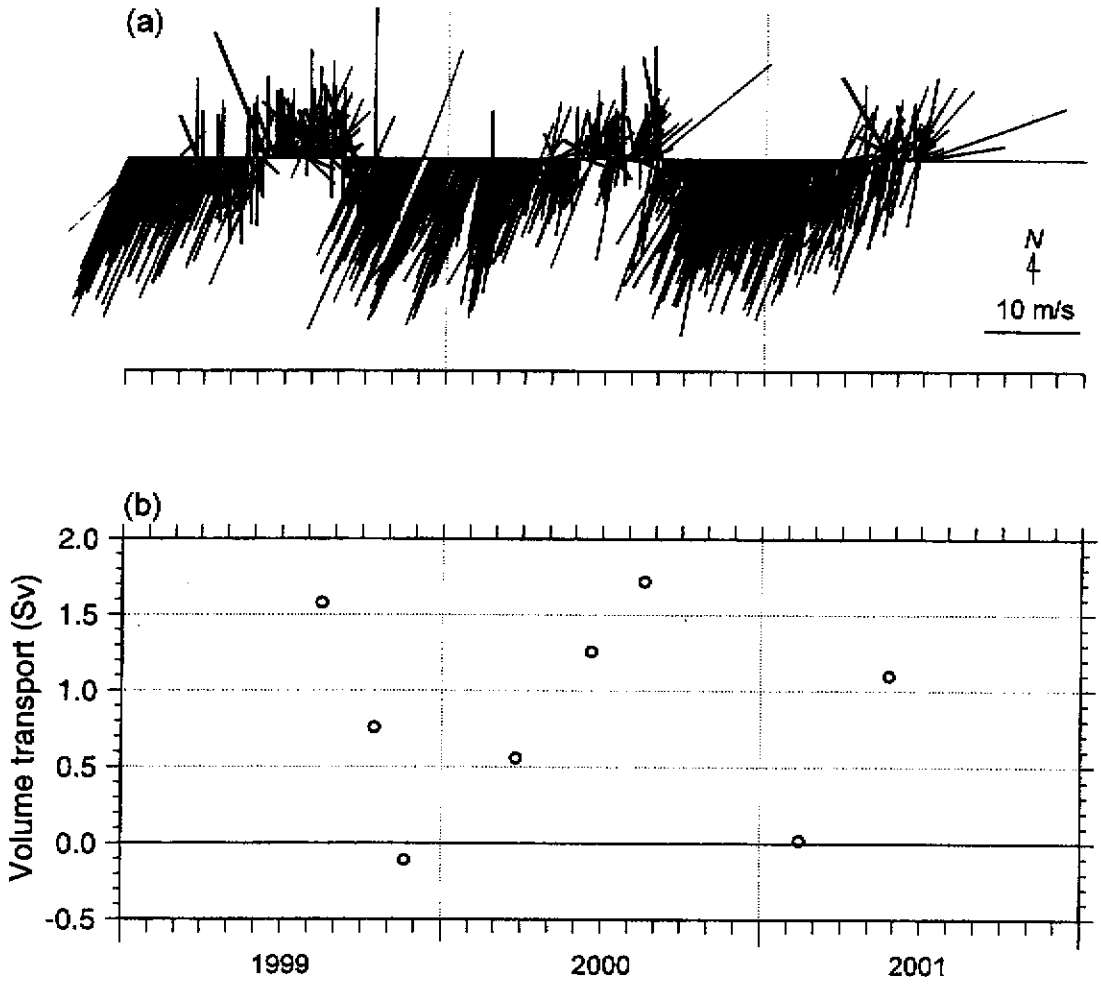

Jan, Chao and Wang Fig. 6

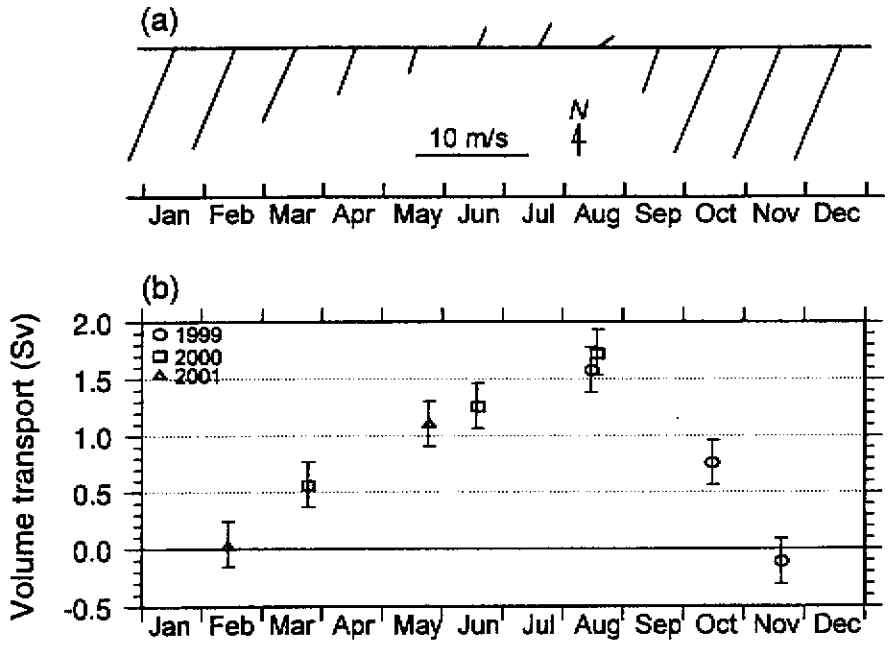

Jan, Chao and Wang Fig. 7